







# Increased bundle-sheath leakiness of CO<sub>2</sub> during photosynthetic induction shows a lack of coordination between the C<sub>4</sub> and C<sub>3</sub> cycles

Yu Wang<sup>1,2\*</sup> , Samantha S. Stutz<sup>1\*</sup> , Carl J. Bernacchi<sup>2,3,4</sup> , Ryan A. Boyd<sup>1</sup> , Donald R. Ort<sup>1,2,4</sup>  and Stephen P. Long<sup>1,2,4,5</sup> 

<sup>1</sup>The Carl R. Woese Institute for Genomic Biology, University of Illinois Urbana-Champaign, 1206 W Gregory Dr, Urbana, IL 61801, USA; <sup>2</sup>DOE Center for Advanced Bioenergy and Bioproducts Innovation, University of Illinois at Urbana-Champaign, Urbana, IL 61801, USA; <sup>3</sup>USDA-ARS Global Change and Photosynthesis Research Unit, University of Illinois at Urbana-Champaign, Urbana, IL 61801, USA; <sup>4</sup>Departments of Plant Biology and Crop Sciences, University of Illinois at Urbana-Champaign, Urbana, IL 61801, USA; <sup>5</sup>Lancaster Environment Centre, Lancaster University, Lancaster, LA1 4YQ, UK

Author for correspondence:  
Stephen P. Long  
Email: slong@illinois.edu

Received: 2 April 2022  
Accepted: 25 August 2022

New Phytologist (2022)  
doi: 10.1111/nph.18485

**Key words:** bundle-sheath leakage, C<sub>4</sub> photosynthesis, carbon isotope discrimination, maize, photosynthetic efficiency, photosynthetic induction, sorghum, tunable diode laser absorption spectroscopy.

## Summary

- Use of a complete dynamic model of NADP-malic enzyme C<sub>4</sub> photosynthesis indicated that, during transitions from dark or shade to high light, induction of the C<sub>4</sub> pathway was more rapid than that of C<sub>3</sub>, resulting in a predicted transient increase in bundle-sheath CO<sub>2</sub> leakiness ( $\phi$ ).
- Previously,  $\phi$  has been measured at steady state; here we developed a new method, coupling a tunable diode laser absorption spectroscope with a gas-exchange system to track  $\phi$  in sorghum and maize through the nonsteady-state condition of photosynthetic induction.
- In both species,  $\phi$  showed a transient increase to > 0.35 before declining to a steady state of 0.2 by 1500 s after illumination. Average  $\phi$  was 60% higher than at steady state over the first 600 s of induction and 30% higher over the first 1500 s.
- The transient increase in  $\phi$ , which was consistent with model prediction, indicated that capacity to assimilate CO<sub>2</sub> into the C<sub>3</sub> cycle in the bundle sheath failed to keep pace with the rate of dicarboxylate delivery by the C<sub>4</sub> cycle. Because nonsteady-state light conditions are the norm in field canopies, the results suggest that  $\phi$  in these major crops in the field is significantly higher and energy conversion efficiency lower than previous measured values under steady-state conditions.

## Introduction

Photosynthetic energy conversion efficiency ( $\epsilon_c$ ), the efficiency with which crops convert intercepted radiation into biomass, is a major limitation to the yield potential for both C<sub>3</sub> and C<sub>4</sub> crops (Zhu *et al.*, 2008, 2010; Long *et al.*, 2015). The  $\epsilon_c$  of C<sub>4</sub> species has the intrinsic advantage of minimizing energy loss to photorespiration under most conditions, compared with C<sub>3</sub> species (Long & Spence, 2013). Although only 3% of species use the C<sub>4</sub> pathway, they account for 23% of terrestrial gross primary productivity (Sage *et al.*, 2012). C<sub>4</sub> species are also overrepresented in agricultural production in which just three C<sub>4</sub> crops (maize, sugarcane and sorghum) account for 32% of global production (Long & Spence, 2013; FAO *et al.*, 2020). All three are from a single C<sub>4</sub> evolutionary clade, tribe Andropogoneae, and use the NADP malic enzyme (ME) for decarboxylation in the bundle sheath. Despite high productivity, even under optimum

conditions, these C<sub>4</sub> crops still fall well short of the theoretical maximum energy conversion efficiency of 6% in the field (Zhu *et al.*, 2008, 2010; Dohleman & Long, 2009). Understanding the limitations to realizing the theoretical maximum in field conditions is key to increasing the productivity of C<sub>4</sub> crops.

C<sub>4</sub> photosynthesis includes a light energy-driven CO<sub>2</sub>-concentrating mechanism that increases the CO<sub>2</sub> concentration around Ribulose-1,5-bisphosphate carboxylase/oxygenase (Rubisco) in bundle-sheath cells, competitively inhibiting the oxygenation reaction, with the result that photorespiration is almost eliminated under normal conditions (Hatch, 1978, 1987; Edwards & Walker, 1983; Keeley & Rundel, 2003; Sage, 2004). Compared with C<sub>3</sub> photosynthesis, C<sub>4</sub> photosynthesis requires two additional ATP per CO<sub>2</sub> assimilated in the regeneration of phosphoenolpyruvate (PEP), the initial acceptor molecule for CO<sub>2</sub> in the mesophyll. However, as the bundle sheath is not hermetically sealed, an inevitable consequence of the high [CO<sub>2</sub>] gradient formed between bundle sheath and mesophyll cells is leakiness ( $\phi$ ). Leakiness describes the proportion of carbon fixed

\*These authors contributed equally to this work.

by PEP carboxylase (PEPC) and released by decarboxylation in the bundle sheath that diffuses back to the mesophyll. A variety of methods have estimated an average  $\phi$  of 0.2 in  $C_4$  NADP-ME species when measured at steady state in high light (Kromdijk *et al.*, 2014). This means that for every five  $CO_2$  molecules released by decarboxylation of malate in the bundle sheath, one will diffuse back to the mesophyll, raising the cost per net  $CO_2$  assimilated by 0.5 ATP. Minimizing  $\phi$  requires close coordination between the  $C_3$  and  $C_4$  cycles. Any elevation of  $\phi$  indicates some lack of coordination between the two photosynthetic cycles and therefore a loss of photosynthetic efficiency (Henderson *et al.*, 1992).

Although previous studies of  $C_4$  leakiness have focused on steady-state conditions (Bellasio & Griffiths, 2014; Kromdijk *et al.*, 2014; von Caemmerer & Furbank, 2016), leaves in crop fields are seldom under steady-state conditions; instead these crop species experience frequent fluctuations in environmental conditions, especially light intensity. Intermittent cloud cover, the movement of leaves, and the changing solar angle over the course of a day cause dramatic and often abrupt changes in the light environment, including sunflecking within the crop canopy (Pearcy, 1990; Zhu *et al.*, 2004; Slattery *et al.*, 2018; Ohkubo *et al.*, 2020; Sakoda *et al.*, 2020; Wang *et al.*, 2020; Qiao *et al.*, 2021; Long *et al.*, 2022). The planting densities of these crops are increasing such that self-shading and more frequent light fluctuations will continue to increase. Although light fluctuations at points on a leaf can occur in fractions of a second, the photosynthetic apparatus may require many minutes to adjust, potentially leading to losses of efficiency at the crop canopy level. This has led to a growing awareness of the need to address photosynthetic efficiency in fluctuating light (Hubbart *et al.*, 2012; McAusland *et al.*, 2016; Deans *et al.*, 2019; Acevedo-Siaca *et al.*, 2020; De Souza *et al.*, 2020; McAusland & Murchie, 2020; Murchie & Ruban, 2020). Much progress has been made in understanding the dynamic response to light in  $C_3$  plants in the past few years. Photosynthetic induction of  $C_3$  plants during shade-to-sun transitions is mainly influenced by three factors: activation of Rubisco, the speed of stomatal opening, and activation of the enzymes involved in RuBP regeneration within the  $C_3$  cycle (Pearcy, 1994; Mott & Woodrow, 2000; Kaiser *et al.*, 2016; Slattery *et al.*, 2018; Taylor *et al.*, 2022). Photosynthetic rate during induction is lower than that under steady-state; however, the major factors limiting photosynthesis, primarily Rubisco activation and stomatal opening, vary among crop species and all represent a loss of potential efficiency (McAusland *et al.*, 2016; Taylor & Long, 2017; Acevedo-Siaca *et al.*, 2020, 2021; De Souza *et al.*, 2020).

When grown under fluctuating light, two  $C_4$  species (*Setaria macrostachya* and *Amaranthus caudatus*) showed a greater reduction in biomass than that observed in two  $C_3$  species (*Triticum aestivum* and *Celosia argentea*) relative to growth under steady-state light (Kubásek *et al.*, 2013). As rapid stomatal movement was reported in  $C_4$  plants (Bellasio *et al.*, 2017; Ozeki *et al.*, 2022), the biomass reduction suggests that  $C_4$  species may be more vulnerable to efficiency losses under fluctuating light, perhaps because of the need to coordinate between the two

photosynthetic cycles. This finding was challenged by Lee *et al.* (2022) who compared carbon assimilation during fluctuating light to steady-state across six  $C_3$  and six  $C_4$  species. Whereas Kubásek *et al.* (2013) made measurements during photosynthetic induction, Lee *et al.* (2022) examined plants that were fully acclimated to high light and suggested that differences between the two studies could be a result of photosynthetic induction causing lower coordination between  $C_3$  and  $C_4$  cycles.

A dynamic modeling simulation of  $C_4$  photosynthetic induction coupled with gas-exchange measurements identified Rubisco activase, PPK regulatory protein and stomatal conductance as the major limitations to the efficiency of NADP-ME-type photosynthesis during dark to high-light fluctuations. The degree of influence of these limiting factors varied somewhat among single accessions of maize, sorghum and sugarcane (Wang *et al.*, 2021). Owing to the complex compartmentation of the photosynthetic reactions between mesophyll and bundle-sheath cells, the gas-exchange measurements in Wang *et al.* (2021) were not able directly to investigate the relationship between the  $C_4$  and  $C_3$  cycles or determine leakiness during induction. However, a higher leakiness was predicted during induction compared with the steady state, as activation of the  $C_4$  dicarboxylate cycle appeared significantly faster than that of Rubisco in the bundle sheath, based on available kinetic data (Wang *et al.*, 2021).

Steady-state  $\phi$  increases only slightly with decreasing light and varies little when measured at different  $[CO_2]$ , suggesting the  $C_3$  and  $C_4$  cycles are well coordinated under steady-state conditions (Henderson *et al.*, 1992; Ubierna *et al.*, 2011, 2013; Bellasio & Griffiths, 2014; Kromdijk *et al.*, 2014). However, little is known about how  $\phi$  changes under nonsteady-state conditions. Leakiness can be estimated by including measurements of photosynthetic carbon isotope discrimination (Kromdijk *et al.*, 2014). Estimates of leakiness using stable isotopes compare the theoretical model of photosynthetic discrimination ( $\Delta^{13}C$ ) (Farquhar, 1983; Farquhar & Cernusak, 2012) with measured photosynthetic discrimination ( $\Delta^{13}C_{obs}$ ) (Kromdijk *et al.*, 2014). Stable isotope discrimination can be estimated in real-time using a tunable diode laser absorption spectroscope (TDL) coupled to a gas-exchange system (Barbour *et al.*, 2007). In steady-state measurements of  $\phi$ , the TDL cycles through a set of calibration gases, and the infrared gas analyzer (IRGA) reference and leaf chamber. The TDL remains on each sample for a period of *c.* 30 s, thus allowing a single measurement every *c.* 120–360 s, precluding continuous monitoring of the leaf chamber. Recently, Sakoda *et al.* (2021) and Liu *et al.* (2022) estimated mesophyll conductance in  $C_3$  plants through induction using the steady-state TDL method and were only able to measure *c.* 15 data points over a 30 min activation curve.

Here, we developed an experimental design that measures  $\phi$  every *c.* 10 s over a 30 min induction. Based on our previous metabolic modeling (Wang *et al.*, 2021) we hypothesized that leakiness will be higher during activation of  $C_4$  photosynthesis than during steady-state conditions. The hypothesis is tested directly here from near-continuous  $\Delta^{13}C$  discrimination measurements through induction of photosynthesis in maize and sorghum.

## Materials and Methods

### Plant material and growth conditions

Sorghum (*Sorghum bicolor* L. Moench, Tx430) and maize (*Zea mays* L., B73) plants were grown in a controlled-environment glasshouse at the University of Illinois at Urbana-Champaign. Temperature in the glasshouse was 28°C : 24°C, day : night. Plants were grown in 20 l pots filled with peat-and-perlite growing medium (BM6; Berger, Saint-Modeste, QC, Canada). Measurements were taken on plants at 40 d after planting. Plants were kept in darkness for  $\geq 30$  min before measurement. The youngest fully expanded leaf on the main stem, as indicated by a fully emerged ligule, was selected for enclosure into the controlled-environment measurement chamber.

### Gas-exchange measurements

For sorghum, the leaf was placed in the opaque conifer chamber (LI-6400-22; Li-Cor Environmental, Lincoln, NE, USA) with an integrated RGB light source (LI-6400-18; Li-Cor Environmental) attached to a LI-6400XT gas-exchange system (Li-Cor Environmental). The chamber was fitted with a leaf thermocouple (Omega Engineering Inc., Norwalk, CT, USA) (Fig. S1a). To minimize leakage from the chamber, an opaque flexible polymer sealant (Qubitac Sealant; Qubit Systems Inc., Kingston, ON, Canada) was applied around the chamber lips after enclosing the leaf (Fig. S1a). For maize, the leaf was placed in the large leaf and needle chamber (LI-6800-13; Li-Cor Environmental) incorporating the large light source (LI-6800-03; Li-Cor Environmental) (Fig. S1b). The flows to the reference and sample IRGAs were monitored to ensure that both analyzers received sufficient flow. Because maize has a large midvein, the sample chamber pressure was set to 0.1 kPa to ensure that any leaks were out of, not into, the sample chamber. The average ( $\pm$ SE) leakage from the chamber from all the maize measurements was  $6.4 \pm 1.9 \mu\text{mol s}^{-1}$ , which accounted for  $2.1 \pm 0.68\%$  of the flow. For both species, the leaf was placed in the chamber in darkness with a leaf temperature of 27°C, CO<sub>2</sub> reference of  $800 \mu\text{mol mol}^{-1}$ , an [O<sub>2</sub>] of 21% and a flow rate of  $300 \mu\text{mol s}^{-1}$ . We controlled reference [CO<sub>2</sub>] to avoid artifacts caused by system adjustment. Reference CO<sub>2</sub> of  $800 \mu\text{mol mol}^{-1}$  was used to ensure that the sample [CO<sub>2</sub>] during the measurement is not lower than the ambient CO<sub>2</sub>. Leaf area was calculated as the product of the internal length of the chamber and the average of the width of the leaf at both ends of the chamber.

### Isotopic gas-exchange measurement

The gas-exchange system was coupled to a TDL (model TGA 200A; Campbell Scientific Inc., Logan, UT, USA) to measure [<sup>12</sup>CO<sub>2</sub>], [<sup>13</sup>CO<sub>2</sub>] and  $\delta^{13}\text{C}$  (Bowling *et al.*, 2003; Pengelly *et al.*, 2010; Ubierna *et al.*, 2013; Jaikumar *et al.*, 2021). For sorghum, the reference line for the LI-6400XT was split on the back of the sensor head so that a portion of the reference gas was diverted to the TDL. The exhaust gas from the leaf chamber was

taken from the match port on the chamber, fitted with a three-way valve to allow the gas to go to either the TDL or the match valve on the LI-6400XT (Fig. S1a). For maize, the TDL was connected to the LI-6800 reference air stream using the reference port on the back of sensor head while the port on the front of the head supplied air from the leaf chamber (Jaikumar *et al.*, 2021; Fig. S1b). CO<sub>2</sub>-free air (N<sub>2</sub>/O<sub>2</sub>) with a known [O<sub>2</sub>] was created by mixing two gas streams using precision mass flow controllers (Omega Engineering Inc.). A portion of this N<sub>2</sub>/O<sub>2</sub> air traveled to the gas-exchange system while the remainder was used as CO<sub>2</sub>-free air in calibration to correct for drift in the TDL over the course of the measurements. The TDL was calibrated using the concentration series method by diluting a 10% CO<sub>2</sub> gas cylinder into the N<sub>2</sub>/O<sub>2</sub> stream to produce three different [CO<sub>2</sub>] of the same isotopic composition (Pengelly *et al.*, 2010; Tazoe *et al.*, 2011; Ubierna *et al.*, 2013; Jaikumar *et al.*, 2021). The measurement sequence cycled through eight gas streams in the following sequence: CO<sub>2</sub>-free air, followed by three different CO<sub>2</sub> concentrations of the same isotopic signature, air from a calibration tank with a known [<sup>12</sup>CO<sub>2</sub>], [<sup>13</sup>CO<sub>2</sub>], and  $\delta^{13}\text{C}$  composition (NOAA Global Monitoring Laboratory, Boulder, CO, USA), the IRGA reference and leaf chamber air streams, and the IRGA reference again. Each step had a duration of 20 s, except for the leaf chamber air, which had a duration of 600 s with a total cycle time of 740 s. Measurements were collected at a 10 Hz interval and averaged over 10 s as a single data point. The first 10 s of each gas stream was excluded to produce a single data point, except for the sample line which produced 59 data points each cycle. Instrument performance, including Allan deviations and instrument precision, are presented in Notes S1.

When the TDL switched to measuring the gas from the leaf chamber, the irradiance incident on the leaf was changed from 0 to  $1800 \mu\text{mol quanta m}^{-2} \text{ s}^{-1}$ . The gas-exchange system was set to auto-log at 10 s intervals over the course of 30 min. Dark respiration rate was recorded before illumination.

### Calculations of photosynthetic discrimination ( $\Delta^{13}\text{C}$ ) and leakiness ( $\phi$ )

Instantaneous online determination of observed photosynthetic discrimination ( $\Delta^{13}\text{C}_{\text{obs}}$ ; Table 1) was calculated according to Evans & von Caemmerer (2013):

$$\Delta^{13}\text{C}_{\text{obs}} = \frac{1000\xi(\delta^{13}\text{C}_{\text{samp}} - \delta^{13}\text{C}_{\text{ref}})}{1000 + \delta^{13}\text{C}_{\text{samp}} - \xi(\delta^{13}\text{C}_{\text{samp}} - \delta^{13}\text{C}_{\text{ref}})} \quad \text{Eqn 1}$$

where  $\delta^{13}\text{C}_{\text{samp}}$  and  $\delta^{13}\text{C}_{\text{ref}}$  are the carbon isotope compositions of the leaf chamber and reference air, respectively, and  $\xi$  is:

$$\xi = \frac{C_{\text{ref}}}{C_{\text{ref}} - C_{\text{samp}}} \quad \text{Eqn 2}$$

$C_{\text{ref}}$  and  $C_{\text{samp}}$  are the [CO<sub>2</sub>] of dry air entering and exiting the leaf chamber, respectively, as measured by the TDL. For each measurement sequence, we averaged the [CO<sub>2</sub>] and  $\delta^{13}\text{C}$  of the

**Table 1** List of symbols used in the text for calculating leakiness in maize and sorghum.

Variable	Definition	Units	Equations/value/reference
$a$	Fractionation across the stomata	‰	4.4 (Craig, 1953; $a_s$ in Ubierna <i>et al.</i> , 2013, 2018)
$a_b$	Fractionations across the boundary layer	‰	2.9
$\bar{a}$	Weighted fractionation across the boundary layer and stomata in series	‰	Eqn 18 (Ubierna <i>et al.</i> , 2013, 2018)
$A$	Rate of photosynthesis	$\mu\text{mol m}^{-2} \text{s}^{-1}$	Measured
$b_3$	$^{13}\text{C}$ fractionation during carboxylation by Rubisco, including respiration and photorespiration fractionations	‰	Eqn 13 (Farquhar, 1983)
$b'_3$	$^{13}\text{C}$ fractionation during carboxylation by Rubisco	‰	30
$b_4$	Net fractionation by $\text{CO}_2$ dissolution, hydration and phosphoenolpyruvate carboxylase (PEPC) including respiratory fractionation	‰	Eqn 14 (Farquhar, 1983)
$b'_4$	Net fractionation by $\text{CO}_2$ dissolution, hydration and PEPC activity dependent upon temperature	‰	Eqn 15
$C_a$	Ambient $\text{CO}_2$ partial pressure	Pa	Measured in $\mu\text{mol mol}^{-1}$ air
$C_{bs}$	$\text{CO}_2$ partial pressure in the bundle-sheath cells	Pa	Eqn 7
$C_i$	$\text{CO}_2$ partial pressure at the intercellular airspace	Pa	Measured in $\mu\text{mol mol}^{-1}$ air
$C_s$	$\text{CO}_2$ partial pressure at the leaf surface	Pa	Measured in $\mu\text{mol mol}^{-1}$ air
$C_{ref}$	$\text{CO}_2$ concentration of the dry air exiting the leaf chamber	$\mu\text{mol mol}^{-1}$	Measured
$C_{samp}$	$\text{CO}_2$ concentration of the dry air exiting the leaf chamber	$\mu\text{mol mol}^{-1}$	Measured
$e$	$^{13}\text{C}$ fractionation during decarboxylation	‰	0 (Evans & von Caemmerer, 2013; Ubierna <i>et al.</i> , 2013)
$e'$	$^{13}\text{C}$ fractionation during decarboxylation including the effect of a respiratory substrate isotopically distinct from recent photosynthate	‰	Eqn 16
$E$	Rate of transpiration	$\text{mol m}^{-2} \text{s}^{-1}$	Measured
$f$	$^{13}\text{C}$ fractionation during photorespiration	‰	1.6‰ (Ubierna <i>et al.</i> , 2013)
$g_{ac}^t$	Total conductance to $\text{CO}_2$ diffusion including boundary layer and stomatal conductance	$\text{mol m}^{-2} \text{s}^{-1}$	Measured
$g_{bs}$	Bundle-sheath conductance to $\text{CO}_2$	$\text{mol m}^{-2} \text{s}^{-1}$	0.00113 (Brown & Byrd, 1993)
$J_t$	Total electron transport rate	$\mu\text{mol m}^{-2} \text{s}^{-1}$	Eqn 3 (von Caemmerer, 2000)
$O_m$	$\text{O}_2$ partial pressure in the mesophyll cells	Pa	21.2 Pa atmospheric pressure
$O_s$	$\text{O}_2$ partial pressure in the bundle-sheath cells	Pa	Eqn 11 (von Caemmerer, 2000)
$R_d$	Leaf mitochondrial respiration in the light assumed to equal the rate of respiration in the dark	$\mu\text{mol m}^{-2} \text{s}^{-1}$	Measured
$R_m$	Rate of mesophyll cell respiration in the light	$\mu\text{mol m}^{-2} \text{s}^{-1}$	$R_m = 0.5R_d$
$s$	Fractionation during leakage from the bundle-sheath cells	‰	1.8 (Henderson <i>et al.</i> , 1992)
$t$	Ternary effect	‰	Eqn 17
$V_c$	Rubisco carboxylation rate	$\mu\text{mol m}^{-2} \text{s}^{-1}$	Eqn 9 (von Caemmerer, 2000)
$V_o$	Rubisco oxygenation rate	$\mu\text{mol m}^{-2} \text{s}^{-1}$	Eqn 10 (von Caemmerer, 2000)
$V_p$	PEP carboxylation rate	$\mu\text{mol m}^{-2} \text{s}^{-1}$	Eqn 8 (von Caemmerer, 2000)
$x$	Fraction of $J_t$ allocated to the $\text{C}_4$ cycle		0.4 (von Caemmerer, 2000)
$\alpha$	Fraction of PSII activity in the bundle sheath		0 (von Caemmerer, 2000)
$\delta^{13}\text{C}_{gatm}$	Isotopic signature of growth $\text{CO}_2$	‰	-8
$\delta^{13}\text{C}_{ref}$	Isotopic signature of the $\text{CO}_2$ entering the leaf chamber	‰	Measured
$\delta^{13}\text{C}_{samp}$	Isotopic signature of the $\text{CO}_2$ exiting the leaf chamber	‰	Measured
$\xi$	Ratio of the $^{12}\text{CO}_2$ mole fraction in the dry air coming into the gas-exchange cuvette over the difference in $^{12}\text{CO}_2$ mole fractions of air in and out of the cuvette	unitless	Eqn 2
$\Delta^{13}\text{C}_{obs}$	Observed $^{13}\text{C}$ photosynthetic discrimination	‰	Eqn 1
$\phi_{is}$	Leakiness estimated assuming infinite mesophyll conductance	Unitless	Eqn 12

reference air measured before and after the measurement of leaf chamber air.

The electron transport flux ( $J_t$ ) was calculated as (von Caemmerer, 2000; Ubierna *et al.*, 2013):

$$J_t = \frac{-II + \sqrt{II^2 - 4 \cdot III \cdot I}}{2 \cdot III} \quad \text{Eqn 3}$$

where

$$I = \left(1 + \frac{R_d}{A}\right) \left(R_m - g_{bs} C_m - \frac{7g_{bs}\gamma^* O_m}{3}\right) + (R_d + A) \left(1 - \frac{7\alpha\gamma^*}{3 \times 0.047}\right) \quad \text{Eqn 4}$$

$$\text{II} = \frac{1-x}{3} \left[ \frac{g_{\text{bs}}}{A} \left( C_m - \frac{R_m}{g_{\text{bs}}} - \gamma^* O_m \right) - 1 - \frac{\alpha \gamma^*}{0.047} \right] - \frac{x}{2} \left( 1 + \frac{R_d}{A} \right)$$

Eqn 5

$$\text{III} = \frac{x-x^2}{6A}$$

Eqn 6

$R_d$  is leaf mitochondrial respiration in the light, assumed to be equal to dark respiration,  $R_m$  ( $R_m = 0.5R_d$ ) is the rate of mesophyll cell respiration in the light, and  $A$  is the rate of net  $\text{CO}_2$  assimilation.  $C_m$  is  $\text{CO}_2$  concentration in the mesophyll cells, which was assumed to equal measured  $C_i$ ,  $\gamma^*$  is half of the reciprocal of Rubisco specificity (0.000193; von Caemmerer *et al.*, 1994),  $O_m$  is the  $\text{O}_2$  mol fraction in the mesophyll cells ( $210\,000\ \mu\text{mol mol}^{-1}$ ), and  $x$  is the portion of ATP used by the  $C_4$  cycle, assumed to equal 0.4 (von Caemmerer, 2000). The fraction of PSII activity in the bundle sheath ( $\alpha$ ) was assumed to be 0 for maize and sorghum (von Caemmerer, 2000). The bundle-sheath conductance to  $\text{CO}_2$  ( $g_{\text{bs}}$ ) was set as  $0.00113\ \text{mol m}^{-2}\ \text{s}^{-1}$  (Brown & Byrd, 1993).

We calculated the  $\text{CO}_2$  partial pressure in the bundle-sheath cells ( $C_s$ ), PEP carboxylation rate ( $V_p$ ), Rubisco carboxylation rate ( $V_c$ ), oxygenation rate ( $V_o$ ) and the  $\text{O}_2$  partial pressure in the bundle-sheath cells ( $O_s$ ) using the following expressions (von Caemmerer, 2000):

$$C_{\text{bs}} = \frac{\gamma^* O_s \left[ \frac{7}{3}(A + R_d) + \frac{(1-x)J_t}{3} \right]}{\frac{(1-x)J_t}{3} - (A + R_d)}$$

Eqn 7

$$V_p = \frac{xJ_t}{2}$$

Eqn 8

$$V_c = \frac{A + R_d}{1 - \frac{\gamma^* O_s}{C_{\text{bs}}}}$$

Eqn 9

$$V_o = \frac{V_c - A - R_d}{0.5}$$

Eqn 10

$$O_s = \frac{\alpha A}{0.047 g_{\text{bs}}} + O_m$$

Eqn 11

We estimated leakiness, assuming infinite mesophyll conductance, using the model proposed by Ubierna *et al.* (2013):

$$\phi_{\text{is}} = \frac{C_{\text{bs}} - C_i}{C_i} \frac{(1-t)\Delta^{13}\text{C}_{\text{obs}} C_a - d'(C_a - C_i) - (1+t)C_i b_4}{(1+t)[b_3 C_{\text{bs}} - s(C_{\text{bs}} - C_i)] + d'(C_a - C_i) - (1-t)\Delta^{13}\text{C}_{\text{obs}} C_a}$$

Eqn 12

where  $C_a$ , and  $C_i$  are the ambient and intercellular  $\text{CO}_2$  partial pressures, respectively, and  $t$  is the ternary effect (Farquhar &

Cernusak, 2012). The fractionation during leakage from the bundle-sheath cells ( $s$ ) is 1.8‰, and  $b_3$  and  $b_4$  were defined as (Farquhar, 1983):

$$b_3 = b'_3 - \frac{e' R_d}{V_c} - \frac{f V_o}{V_c}$$

Eqn 13

$$b_4 = b'_4 - \frac{e' R_m}{V_p}$$

Eqn 14

where  $f$  is fractionation during photorespiration, assumed to be 11.6‰ (Lanigan *et al.*, 2008).  $b'_3$  (30‰) is Rubisco fractionation, and  $b'_4$ , the net fractionation by  $\text{CO}_2$  dissolution, hydration and PEP activity at 27°C, was calculated according to Mook *et al.* (1974), which is used by Henderson *et al.* (1992) and von Caemmerer *et al.* (2014):

$$b'_4 = \frac{-9.483 \times 1000}{273 + (T^\circ\text{C})} + 23.89 + 2.2$$

Eqn 15

We estimated  $e'$ , which is the  $^{13}\text{CO}_2$  fractionation during decarboxylation and takes into account respiration that is isotopically distinct from recent photosynthate, as previously discussed (Wingate *et al.*, 2007; Ubierna *et al.*, 2018):

$$e' = e + \delta^{13}\text{C}_{\text{ref}} - \delta^{13}\text{C}_{\text{g atm}}$$

Eqn 16

where  $e$  is the respiratory fractionation during decarboxylation, 0‰,  $\delta^{13}\text{C}_{\text{g atm}}$  is the isotopic signature of the  $\text{CO}_2$  in the air where the plants were grown, assumed to be -8‰, and  $\delta^{13}\text{C}_{\text{ref}}$  is the isotopic signature of the measurement  $\text{CO}_2$  and was between -10‰ and -6.5‰.

The ternary effect ( $t$ ) (Farquhar & Cernusak, 2012) takes into account the effect of transpiration on the rate of  $\text{CO}_2$  assimilation through the stomata and is calculated as:

$$t = \frac{(1+d')E}{2g_{\text{ac}}^t}$$

Eqn 17

where  $E$  is the rate of transpiration,  $g_{\text{ac}}^t$  is the total conductance to  $\text{CO}_2$  diffusion from the atmosphere to the intercellular airspace including boundary layer and stomatal conductance (von Caemmerer & Farquhar, 1981), and  $d'$  denotes the combined fractionation factor through the leaf boundary layer and the stomata:

$$d' = \frac{a_b(C_a - C_s) + a(C_s - C_i)}{C_a - C_i}$$

Eqn 18

where  $C_s$  is the leaf surface  $\text{CO}_2$  partial pressure,  $a_b$  (2.9‰) is the fractionation occurring through diffusion in the boundary layer, and  $a$  (4.4‰) is the fractionation as a result of diffusion in air (Craig, 1953).

### The error associated with $\Delta^{13}\text{C}_{\text{obs}}$ measurements

The error associated with  $\Delta^{13}\text{C}_{\text{obs}}$  was calculated according to Ubierna *et al.* (2018):

$$\text{Error} = \sqrt{2} \xi X \quad \text{Eqn 19}$$

where  $X$  is instrument precision (Notes S1). The error (%) was calculated as  $\text{error}(\%) = (\text{error}/\Delta^{13}\text{C}_{\text{obs}}) \times 100$ .

Instrument precisions during the measurements were 0.24‰ and 0.14‰ for sorghum and maize, respectively. We excluded all data points where the error in  $\Delta^{13}\text{C}_{\text{obs}}$  was > 50%. This occurred in the first 144 s for sorghum and the first 110 s for maize.

### Data processing

A fully automatic data processing and leakiness calculation tool was developed in MATLAB. The tool used the pretreated (LI-6400XT and LI-6800) data files and the raw TDL data to calculate the leakiness through the photosynthetic induction, with the equations described earlier. The TDL data were averaged every 10 s to match the gas-exchange data and to reduce noise (Fig. S2). See the [Data availability](#) statement for access to this tool.

### Correction of the system delay

System delays were caused by both the large volume of the leaf chambers and the gas path from leaf chamber to the TDL (see Methods S1 for further information). The time delay from leaf chamber to the TDL was estimated by pulsing the leaf chamber with high  $\text{CO}_2$  and monitoring the time it took to observe the  $\text{CO}_2$  spike in the TDL. A 5-cm-wide paper strip was clipped into the chamber sealed with opaque flexible polymer sealant (Qubitac Sealant) to mimic the effect of the leaf on flow and mixing. The  $[\text{CO}_2]$  was recorded every 2 s until the chamber outlet  $[\text{CO}_2]$  was stable at  $400 \mu\text{mol mol}^{-1}$  (Fig. S3). Three different flow rates were measured, 300, 500 and  $700 \mu\text{mol s}^{-1}$ . For each flow rate, the measurements were repeated three times. Results were used to estimate the chamber volume ( $V_{\text{chamber}}$ ) and time constant ( $\tau$ ), as defined later (<https://www.licor.com/env/support/LI-6400/topics/custom-chamber.html>).

Assuming the gas is well mixed in the chamber, for an open, flow-through system, the  $[\text{CO}_2]$  in the chamber  $C(t)$  at time  $t$  is:

$$C(t) = C_{\text{in}} - (C_{\text{in}} - C_0) e^{-\frac{f V_{\text{m}}}{V_{\text{chamber}}} t} \quad \text{Eqn 20}$$

where  $C_0$  is the initial chamber  $[\text{CO}_2]$ ,  $C_{\text{in}}$  is the incoming  $[\text{CO}_2]$ ,  $V_{\text{m}}$  is the molar volume of air, which was assumed to approximate an ideal gas at standard atmospheric pressure and  $27^\circ\text{C}$ , and is set as  $24.6 \text{ l mol}^{-1}$ ,  $f$  is the air flow rate (s) and  $V_{\text{chamber}}$  is the chamber volume (l). Then, an ordinary differential equation model was used to estimate the system delay during photosynthetic induction measurement:

$$\frac{dC}{dt} = \frac{S_{\text{leaf}}(A_{\text{leaf}}(C) - A'_{\text{leaf}})}{V_{\text{chamber}}} V_{\text{m}} \quad \text{Eqn 21}$$

where  $S_{\text{leaf}}$  is the leaf area,  $A_{\text{leaf}}(C)$  is the leaf carbon assimilation rate estimated by the gas-exchange system at a given  $[\text{CO}_{2\text{ref}}]$ , and  $A'_{\text{leaf}}$  is the actual carbon assimilation rate. Here we set it as:

$$A'_{\text{leaf}} = A_f \left(1 - e^{-\frac{t}{\tau_A}}\right) \quad \text{Eqn 22}$$

where  $A_f$  is the steady-state photosynthesis rate at high light,  $\tau_A$  is the time constant of the induction of photosynthesis, and  $A_f$  and  $\tau_A$  were set as  $40 \mu\text{mol m}^{-2} \text{ s}^{-1}$  and 300 s, respectively, according to gas-exchange measurements.

### Rubisco activation estimation

If the photosynthetic rate is limited by Rubisco, the maximum Rubisco activity is:

$$V_{\text{cmax}} = A + R_d \quad \text{Eqn 23}$$

Thus, the rate constant of Rubisco activation is equal to the rate constant of induction of  $\text{CO}_2$  assimilation. A semilogarithmic plot of the difference between  $A$  and steady-state  $\text{CO}_2$  assimilation at  $1800 \mu\text{mol m}^{-2} \text{ s}^{-1}$  ( $A_f$ ) as a function of time during photosynthetic induction was plotted (Fig. S4). The linear portion of the semilogarithmic plot reflects an exponential phase in the time course that is proposed to be limited primarily by Rubisco (Woodrow & Mott, 1993; Wang *et al.*, 2021). The slope of this linear portion is equal to the negative reciprocal of the time constant for  $\text{CO}_2$  assimilation and Rubisco activation ( $\tau_A = \tau_{\text{Rubisco}}$ ). As Rubisco limits the later phase of the induction of  $\text{C}_4$  crops, we used the measured photosynthetic rate between 300 and 900 s for this estimation.

### Statistical analyses

Normal distribution and homogeneity of variances were tested by the Shapiro–Wilk and Levene tests, respectively. Student's  $t$ -test was used to determine if the means of two datasets were significantly different from each other ( $P < 0.05$ ). All statistical analyses used PYTHON (v.3.7), Shapiro–Wilk test, Levene test and Student's  $t$ -test were performed using the SCIPY library. The piecewise function was fitted by linear and exponential goodness-to-fit regression (ORIGINPRO v.2020; OriginLab, Northampton, MA, USA).

## Results

### Leakiness during photosynthetic induction in sorghum

During the photosynthetic induction, sample  $[\text{CO}_2]$  declined rapidly from  $820 \mu\text{mol mol}^{-1}$  to a steady state of  $c. 450 \mu\text{mol mol}^{-1}$  at  $c. 600$  s (Fig. 1a). Photosynthetic discrimination ( $\Delta^{13}\text{C}_{\text{obs}}$ ) was used to estimate leakiness ( $\phi$ ), declining from an initial 10‰ to  $c. 3.5$ ‰ at 120 s, then rising to 5‰ at 300 s and finally declining to a steady state of  $c. 2.0$ ‰ at  $c. 1500$  s (Fig. 1b). As expected,  $\xi$ , a measure of the uncertainty in  $\Delta^{13}\text{C}_{\text{obs}}$  was high (15) when rates of photosynthesis were low and decreased as

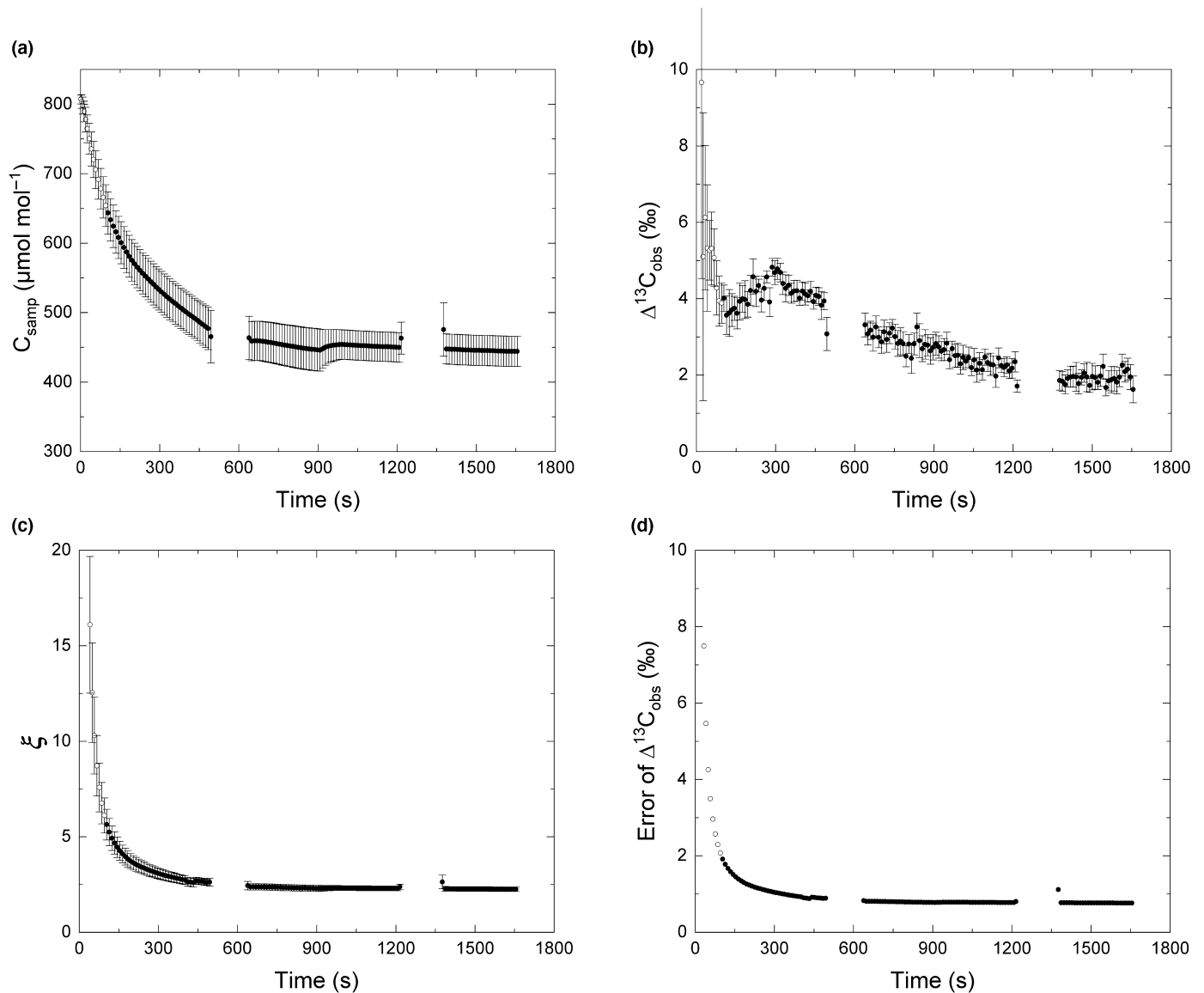


**Fig. 1** Measured carbon isotope discrimination during photosynthetic induction of sorghum (Tx430) using a tunable diode laser absorption spectroscopy (TDL) coupled to a gas-exchange system (LI-6400XT). (a) Sample  $[\text{CO}_2]$ ; (b) the observed leaf photosynthetic discrimination ( $\Delta^{13}\text{C}_{\text{obs}}$ ); (c)  $\xi$ , an estimate of the uncertainty in  $\Delta^{13}\text{C}_{\text{obs}}$  and  $\phi$  calculations; (d) error of  $\Delta^{13}\text{C}_{\text{obs}}$  going from dark to high light ( $1800 \mu\text{mol m}^{-2} \text{s}^{-1}$ ). Time 0 s refers to when the light was switched on. Open dots represent the data points where the error of  $\Delta^{13}\text{C}_{\text{obs}}$  was  $> 50\%$ . The TDL was calibrated after every 600 s of measurement. The gas from leaf chamber was not measured during the calibration and the measurement of reference gas (140 s), which occurred from c. 490 to 640 s and c. 1215 to 1365 s. Leaf gas-exchange and carbon discrimination of the youngest fully expanded leaf was measured on 40-d-old sorghum (Tx430) plant. The leaf was dark-adapted for 30 min before the measurement. Each data point is the mean ( $\pm$ SE) of eight plants ( $n = 8$ ).

$A$  increased through induction, to a steady state of 2.5 at c. 600 s (Fig. 1c). The error of  $\Delta^{13}\text{C}_{\text{obs}}$  was higher than 2‰ (50% of  $\Delta^{13}\text{C}_{\text{obs}}$ ) in the first 100 s of the measurement and quickly declined to around 1.2‰ (30% of  $\Delta^{13}\text{C}_{\text{obs}}$ ) by 200 s (Fig. 1d; Table N1 in Notes S1).

In the first 120 s in high light ( $1800 \mu\text{mol quanta m}^{-2} \text{s}^{-1}$ ), leakiness ( $\phi$ ) in sorghum declined from 0.32 to c. 0.23; however,  $\phi$  then increased to c. 0.35 at 300 s, before gradually decreasing and reaching a steady state of c. 0.18 (Fig. 2b) at c. 1500 s. The leakiness curve was fitted with a piecewise function. No obvious trend was found in the first segment ( $R$ -squared ( $R^2$ ) = 0.098; Fig. 2b), which is also the

segment with the greatest error of  $\Delta^{13}\text{C}_{\text{obs}}$ . The second segment of the piecewise function showed linear growth ( $R^2 = 0.81$ ); during this time the error rapidly declined to  $< 50\%$  of the associated measurement. The third segment was exponential decline ( $R^2 = 0.93$ ; Fig. 2b). The transition time point of the leakiness curve of sorghum occurred at c. 290 s. Excluding the initial 100 s of measurement, given its high error of  $\Delta^{13}\text{C}_{\text{obs}}$ , the average ( $\pm$ SE)  $\phi$  was  $0.237 \pm 0.012$  over the 1500 s period of induction, which was 32% higher than the steady-state  $\phi$  in high light ( $0.180 \pm 0.015$ ,  $P = 0.005$ ; Fig. 4a (see later); Table S1), indicating a substantial loss of efficiency during induction, compared with the

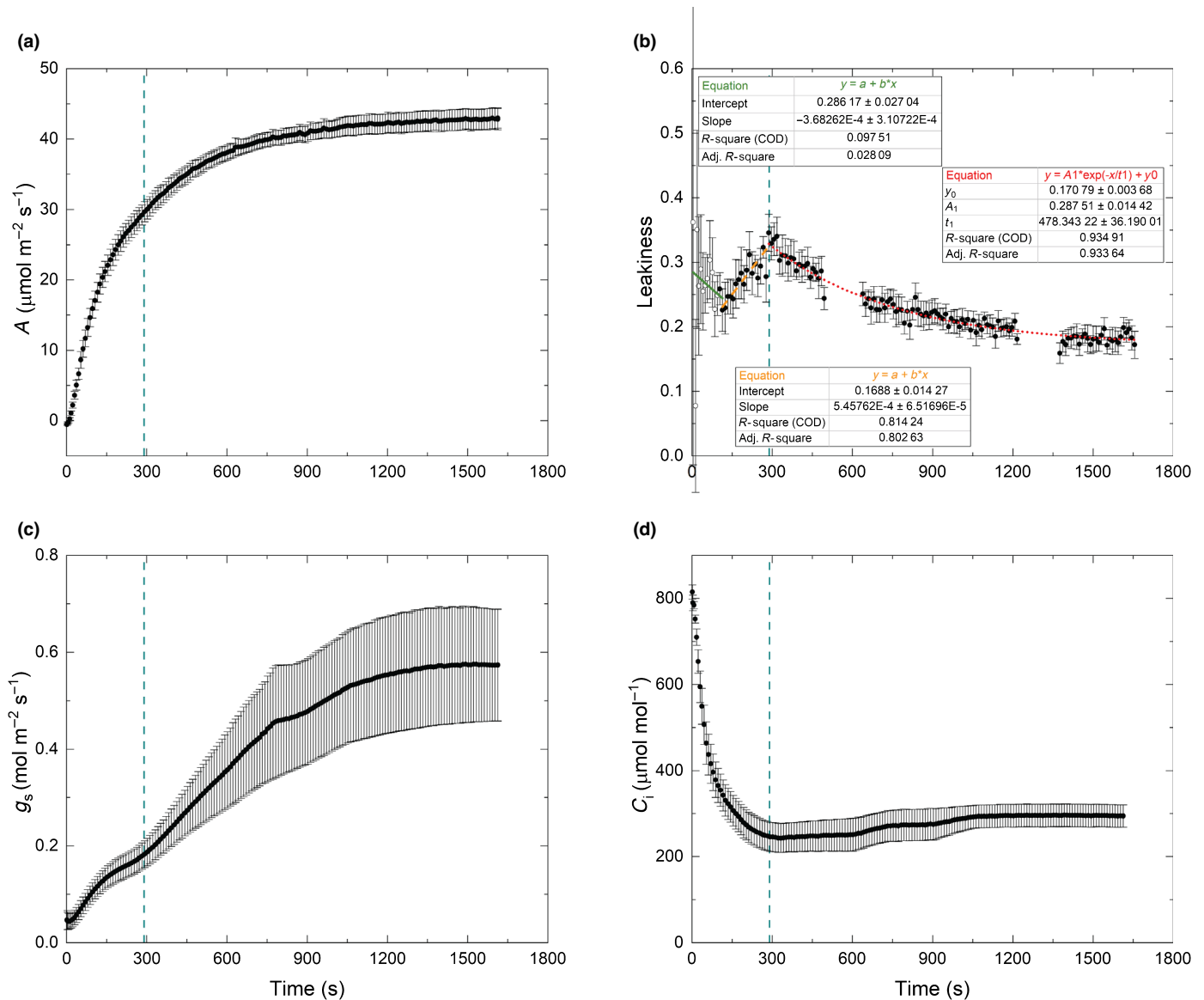


**Fig. 2** CO<sub>2</sub> assimilation and bundle-sheath leakiness during photosynthetic induction of sorghum measured with an LI-6400XT coupled to a tunable diode laser absorption spectroscope (TDL). (a) CO<sub>2</sub> assimilation rate (A). (b) Bundle-sheath leakiness ( $\phi$ , Eqn 12). Open dots represent the data points derived from values of observed discrimination that had large uncertainty (the error in the calculated  $\Delta^{13}\text{C}_{\text{obs}}$  was > 50% of its calculated value). (c) Stomatal conductance to water vapor ( $g_s$ ). (d) Intercellular CO<sub>2</sub> concentration ( $C_i$ ). The dotted vertical lines mark the time of highest leakiness, which was 286 s.  $t_1$  is the time constant ( $\tau$ ) of the exponential curve for leakiness. Time 0 s is when the light was switched on to 1800  $\mu\text{mol m}^{-2} \text{s}^{-1}$ . Each data point is the mean ( $\pm$ SE) of eight plants ( $n = 8$ ).

steady state. The average  $\phi$  value over the first 600 s period of induction was  $0.289 \pm 0.022$ , which was 61% higher than the steady-state  $\phi$  ( $P < 0.001$ ; Fig. 4a (see later); Table S1). The reference [CO<sub>2</sub>] was set as 800  $\mu\text{mol mol}^{-1}$  to minimize the limitations induced by stomatal and mesophyll conductance of CO<sub>2</sub> to PEPC. In sorghum, intercellular [CO<sub>2</sub>] ( $C_i$ ) was always > 200  $\mu\text{mol mol}^{-1}$ , and so assumed not to be limiting to PEP carboxylation (Fig. 2d). Stomatal conductance to water vapor increased from 0.04 to  $\approx 0.57 \text{ mol m}^{-2} \text{s}^{-1}$  through the induction (Fig. 2c). The time constant of photosynthetic induction ( $\tau_A$ ) between 300 and 900 s was 332 s, which was assumed to reflect the kinetics of Rubisco activation (Eqn 21; Fig. S4).

### Leakiness during photosynthetic induction in maize

During the dark to high-light transition, leakiness increased faster in maize than in sorghum (Figs 3b, S8; see later). Similar to the measurement of sorghum, the error associated with  $\Delta^{13}\text{C}_{\text{obs}}$  estimation was > 50% for the first 90 s (Fig. S5d open circles) and photosynthetic discrimination rose rapidly to  $\approx 120$  s before a slow decrease to the steady state (Fig. S5b). As with sorghum,  $\xi$  was high when rates of photosynthesis were low and decreased with increasing rates of assimilation to a steady state at  $\approx 600$  s (Fig. S5c).  $\phi$  during the photosynthetic induction in maize was fitted with the piecewise function. The first segment of the piecewise function was linear growth (Fig. 3b). The first segment of



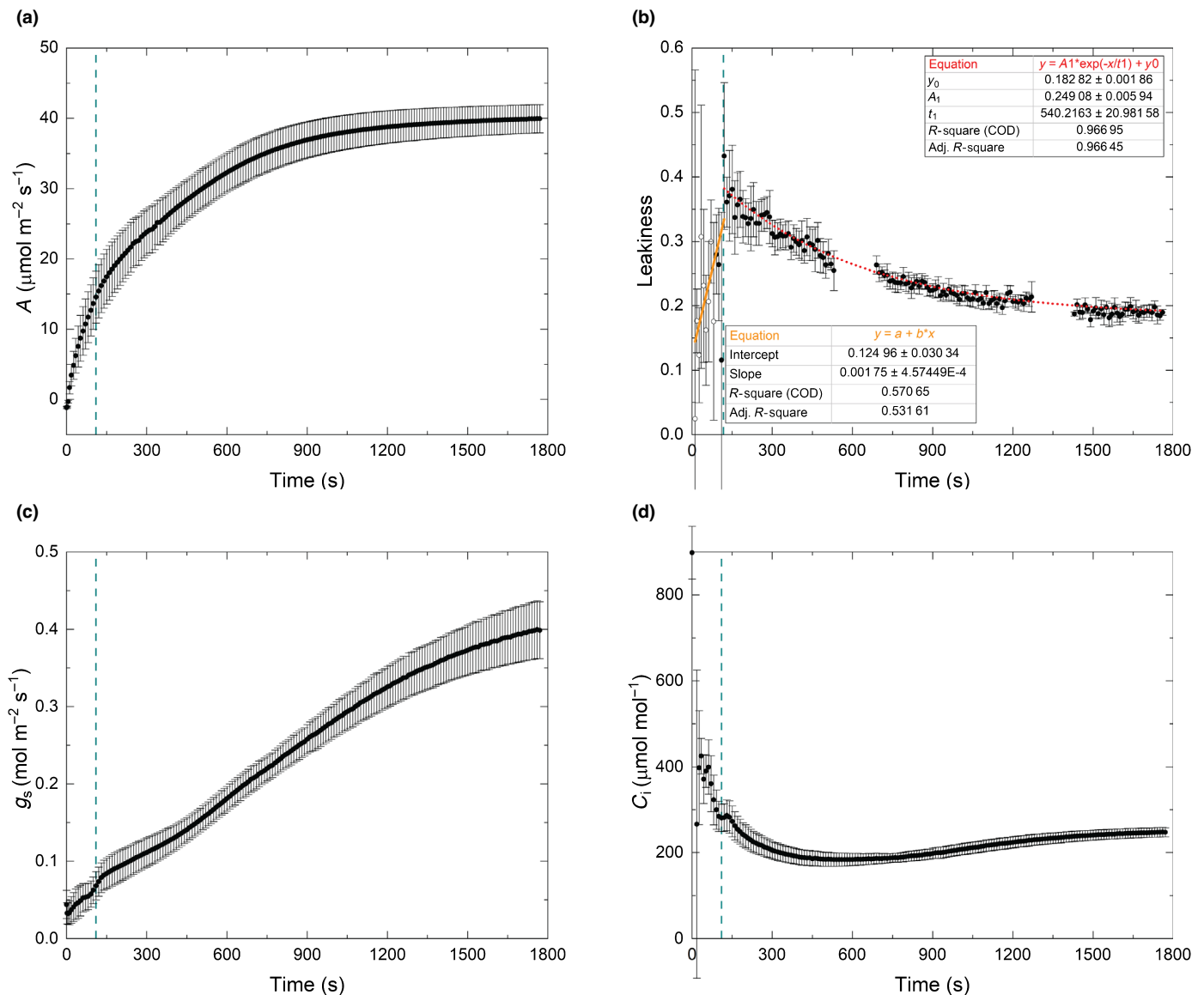


**Fig. 3** CO<sub>2</sub> assimilation and bundle-sheath leakiness during photosynthetic induction of maize B73 measured with an LI-6800 coupled to a tunable diode laser absorption spectroscope (TDL). (a) CO<sub>2</sub> assimilation rate (A). (b) Bundle-sheath leakiness ( $\phi$ , Eqn 12). Open dots represent data points derived from values of observed discrimination that had large uncertainty (the error in the calculated  $\Delta^{13}\text{C}_{\text{obs}}$  was > 50% of its calculated value). (c) Stomatal conductance to water vapor ( $g_s$ ); and (d) intercellular CO<sub>2</sub> concentration ( $C_i$ ). The dotted vertical lines mark the time of highest leakiness, which was 110 s.  $t_1$  is the time constant ( $\tau$ ) of the exponential curve for leakiness. Time 0 is when the light was switched on to  $1800 \mu\text{mol m}^{-2} \text{s}^{-1}$ . The TDL was calibrated after every 600 s of measurement. Each point is the mean ( $\pm$ SE) of six plants.

the piecewise function was linear increase, and  $R^2$  of the linear regression was 0.57; however, the error of  $\Delta^{13}\text{C}_{\text{obs}}$  in this segment is large (Fig. S5d). After 110 s,  $\phi$  during the induction can be fitted with an exponential decline function (Fig. 3b). The time constant of the exponential decline in  $\phi$  was 540 s. The highest  $\phi$  was *c.* 0.4 at 110 s. Excluding the initial 90 s of measurement, given its high error of  $\Delta^{13}\text{C}_{\text{obs}}$ , over the 1500 s period of induction, the average  $\phi$  was  $0.258 \pm 0.006$ , which was 35% higher than the steady-state  $\phi$  at high light ( $0.191 \pm 0.010$ ). Average  $\phi$  over the first 600 s period of induction was  $0.315 \pm 0.014$ , which was 65% higher than the steady state  $\phi$  ( $P < 0.001$ ; Fig. 4b; Table S2). As in the case of sorghum, intercellular [CO<sub>2</sub>] ( $C_i$ ) of maize was always > 200  $\mu\text{mol mol}^{-1}$  (Fig. 3d). Stomatal

conductance to water vapor increased from 0.02 to about 0.4  $\text{mol m}^{-2} \text{s}^{-1}$  through induction (Fig. 3c).

After 1800 s (30 min) in photosynthetic photon flux density of  $1800 \mu\text{mol m}^{-2} \text{s}^{-1}$ , maize and sorghum had similar rates of steady-state CO<sub>2</sub> assimilation and leakiness (Fig. 5a,d), and there was no significant difference between the species in the time taken for A to reach 50% and 90% of the steady-state value, IT50 and IT90, respectively (Fig. 5e,f). However, the rise in leakiness in sorghum was significantly more prolonged than in maize, as indicated by the time taken to reach the peak of leakiness during induction (Fig. 5b). The speed of exponential decay of  $\phi$  was similar, and there was no significant difference between the two species in  $\phi$  (Fig. 5c), which is the time constant of

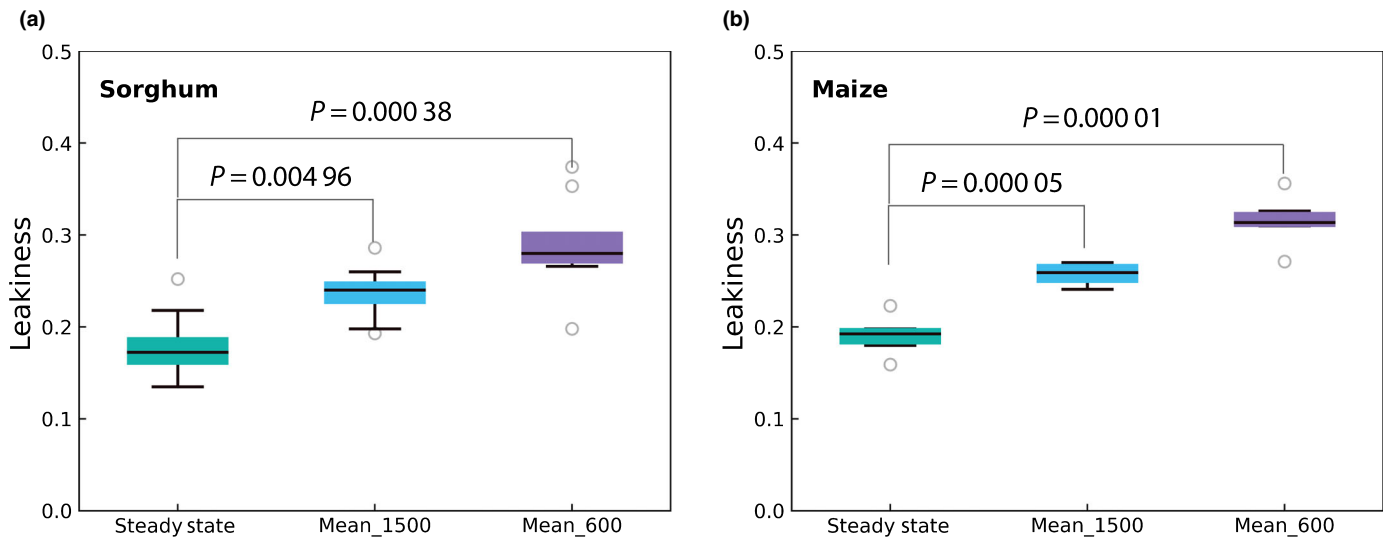


**Fig. 4** The comparison between steady-state and transient leakiness in sorghum (a) and maize (b). Steady state, the average leakiness after 1500 s; Mean\_1500, the average leakiness over the 1500 s period of induction; Mean\_600, the average leakiness of the first 600 s in the induction. The data points with the error of  $\Delta^{13}\text{C}_{\text{obs}} > 50\%$  were excluded. Data of each replicate were listed in Tables S1, S2. *P*-values were calculated using Student's *t*-test. Black circles represent the outliers; black lines in boxes show the medians. Upper and lower whiskers represent the maximum and minimum values, respectively.

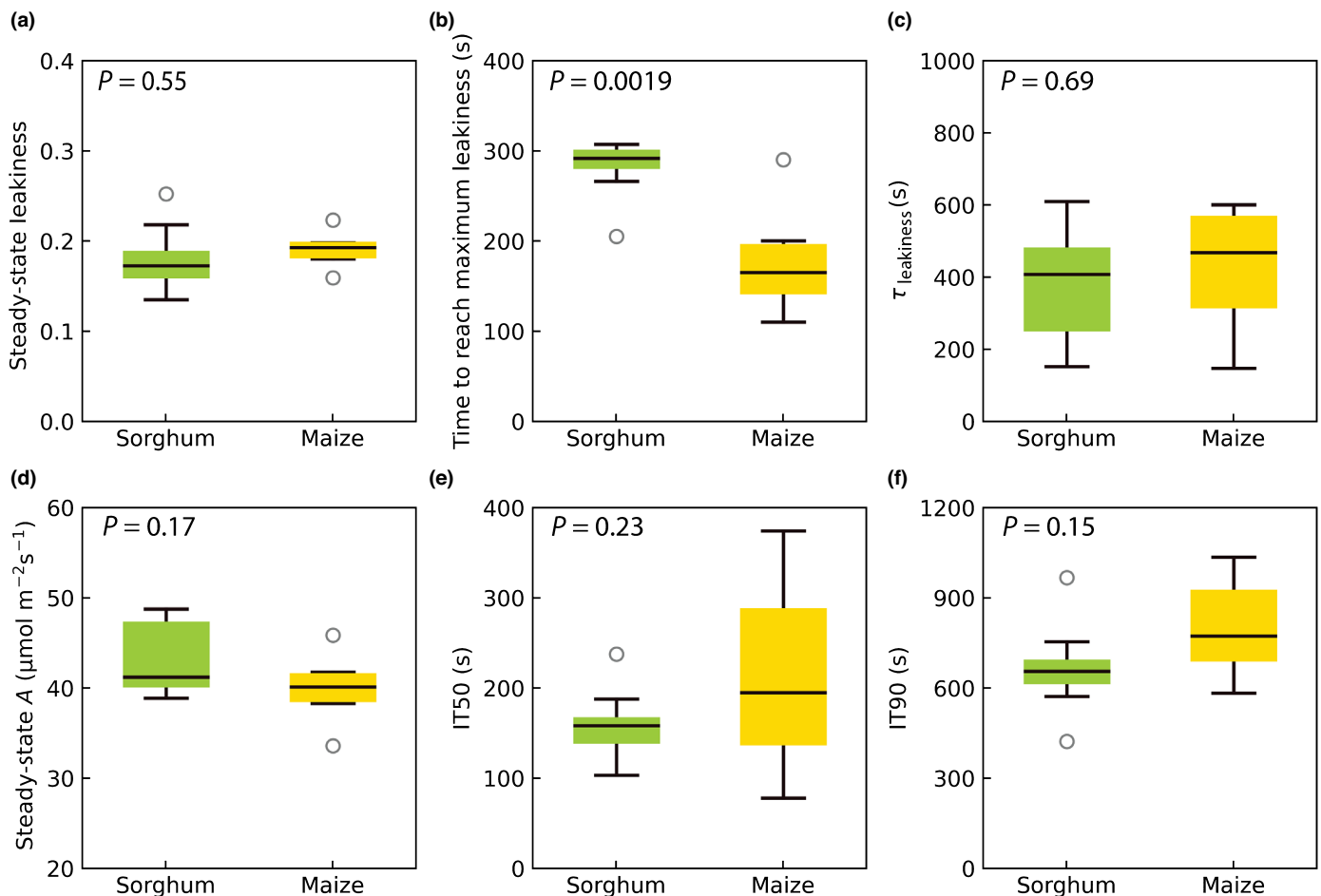


**Fig. 5** Mean and variation of steady-state leakiness, the time to reach the maximum leakiness and the time constant of the exponential decay ( $\tau_{\text{leakiness}}$ ), steady-state  $\text{CO}_2$  assimilation rate (*A*), and IT50 and IT90 during the induction in sorghum and maize. (a) Average leakiness after 1500 s; (b) the time at the end of the linear growth segment of leakiness; (c)  $\tau_{\text{leakiness}}$ , the time constant of exponential decline segment; (d) average *A* after 1500 s; (e) IT50, the time at which *A* reached 50% of the steady state; (f) IT90, the time at which *A* reached 90% of the steady state *A*. *P*-values were calculated using Student's *t*-test. Black circles represent the outliers; black lines in boxes show the medians; upper and lower whiskers represent the maximum and minimum values, respectively.

exponential decline segment of the leakiness function (Figs 2b, 3b; curve-fitting parameter  $\tau_1$ ).

## Discussion

### Coordination between the C<sub>3</sub> and C<sub>4</sub> cycles was disrupted during photosynthetic induction

Coordination between the C<sub>3</sub> and C<sub>4</sub> cycles is essential to the high efficiency of C<sub>4</sub> photosynthesis. We estimated CO<sub>2</sub> leakiness with stable carbon isotopes by coupling a TDL to a gas-exchange system. Leakiness ( $\phi$ ) is the proportion of CO<sub>2</sub> released by decarboxylation of dicarboxylates in the bundle sheath that leaks back to the mesophyll. Any variation in  $\phi$  reflects the degree of coordination between the two cycles.

A complete metabolic model of NADP-ME photosynthesis, incorporating activation of enzymes, stomatal induction and dynamic changes in metabolic pools predicted poor coordination and transient increase in  $\phi$  during photosynthetic induction, as a result of a more rapid activation of PPDK in the mesophyll by the PPDK regulatory protein, than activation of Rubisco in the bundle sheath by Rubisco activase (Wang *et al.*, 2021). The transient increases in  $\phi$  in both maize and sorghum observed here are fully consistent with this explanation.

Leaves in a crop canopy often face intense and rapid light changes (Zhu *et al.*, 2004; Wang *et al.*, 2020; Qiao *et al.*, 2021). Over this 1500 s period of induction, the average  $\phi$  was > 30% higher than the steady-state  $\phi$  at high light for sorghum and maize. Leakiness over the first 600 s was 61% higher than the steady-state  $\phi$  for sorghum and 65% for maize. The lack of coordination between C<sub>4</sub> and C<sub>3</sub> cycles will substantially reduce the efficiency of C<sub>4</sub> photosynthesis at both leaf and canopy levels. Although the present study uses an extreme case of fluctuation (i.e. an immediate transfer from darkness to full sunlight), leaves in the canopy will frequently experience transfer from 10% to full sunlight (Long *et al.*, 2022). A recent application of a high-throughput assay of Rubisco activation has shown that deactivation on transfer to shade is very rapid, occurring within a minute (Taylor *et al.*, 2022). So why has natural selection not removed this inefficiency? In the wild, many C<sub>4</sub> plants, including wild ancestors of maize and sorghum, are most abundant in hot semi-arid and nutrient-poor regions (De Wet, 1978; Yang *et al.*, 2019). As a result, leaf canopies may be sparse, and cloud cover infrequent. In these conditions there will be fewer light fluctuations and little selective pressure to avoid these transient increases in  $\phi$ . The dense modern crop canopies of maize and sorghum are recent in an evolutionary context, but here the losses as a result of these transient inefficiencies would be much greater.

### Differences of transient leakiness between sorghum and maize during induction

The induction rate of CO<sub>2</sub> assimilation was similar between the two species, and a transient increase in leakiness was detected in both sorghum and maize (Figs 2a,b, 3a,b, S6). Leakiness reached a maximum significantly faster in maize than in sorghum (Fig. 5

b), which most probably indicates faster activation of PPDK, possibly as a result of either more of its regulatory protein (PDRP) or a more efficient PDRP (Ashton *et al.*, 1984; Burnell & Chastain, 2006; Wang *et al.*, 2021). These results, consistent with the previous metabolic modeling of NADP-ME C<sub>4</sub> photosynthesis, through induction suggest activation of Rubisco as the key limitation through induction and the primary cause of lost efficiency. Rubisco activase (Rca) appears to be an exceptionally heat-labile protein, implicated in loss of photosynthetic efficiency at high temperatures (Crafts-Brandner & Salvucci, 2000). This implies that the loss of efficiency in these key crops would be amplified by rising global temperatures. This loss of efficiency might be overcome by breeding or engineering an increase in Rca content, and in particular more high-temperature-tolerant isoforms (Carmo-Silva & Salvucci, 2013; Degen *et al.*, 2021). Kim *et al.* (2021). These studies have shown that the redox-regulated Rca- $\alpha$  isoform is expressed in sorghum, sugarcane, maize and *Sateria* only at temperatures > 42°C and the time course of Rca- $\alpha$  corresponds to recovery of Rubisco activation and the rate of photosynthesis from heat shock. However, overall variation in Rca in C<sub>4</sub> crops has so far received little attention. Based on our estimation and previous studies, increasing the activity of Rca by either increasing Rca content or engineering a more efficient Rca would increase photosynthetic efficiency under constant and fluctuating light. Both now appear possible through bioengineering and possibly breeding (Long *et al.*, 2022).

The high CO<sub>2</sub> concentration supplied to the leaf chamber in our experiment (Figs 1a, S6a) minimized diffusional limitations (stomatal and mesophyll) to photosynthesis. During induction, the CO<sub>2</sub> concentrations inside the leaf (C<sub>i</sub>) were > 200 and 180  $\mu\text{mol mol}^{-1}$  for sorghum and maize, respectively (Figs 2d, 3d). Previous research (Wang *et al.*, 2021) demonstrated that at ambient CO<sub>2</sub> concentrations, slow stomatal opening during the middle phase of induction reduced both CO<sub>2</sub> assimilation rate and leakiness in three C<sub>4</sub> crops. The CO<sub>2</sub> concentration used for measurements should have had a negligible effect on leakiness determined for the fast response of stomata in sorghum but could have impacted values for the slower response of stomata seen in maize. Mesophyll conductance ( $g_m$ ) could also be a limiting factor during induction. In this study,  $g_m$  was assumed to be infinite and constant. There are no experimental data on the variation of  $g_m$  during induction in C<sub>4</sub> species. However, the main resistances to CO<sub>2</sub> diffusion through, the cell wall and plasmalemma to the PEP carboxylase bearing mesophyll cytoplasm, are probably unaffected by light, barring a Péclet effect with increasing outflow of water. This is a topic for subsequent investigation.

### Energy-use efficiency of C<sub>4</sub> crops under fluctuating light

The steady-state  $\phi$  values were *c.* 0.2 in maize and sorghum; thus 5.5 ATP are used to assimilate one CO<sub>2</sub>. However, over the 1500 s period of the induction, the average  $\phi$  was 0.25. Moreover, the average  $\phi$  of the first 600 s was *c.* 0.30 in both sorghum and maize. The higher transient  $\phi$  will have increased the ATP consumption of assimilating a CO<sub>2</sub> to 5.7 and 5.9, respectively. The energetic cost of CO<sub>2</sub> assimilation is therefore

higher in fluctuating light than under steady-state conditions. However, when light is in excess, as in induction, this will have little effect.

Variation in carbon assimilation during fluctuating light was previously observed by Lee *et al.* (2022) across four NADP-ME grass species and may well arise from variation in the degree to which the  $C_4$  and  $C_3$  cycles are coordinated, as was shown here for maize and sorghum, but was not determined in their study. Being able to estimate variation in  $\phi$  between species and genotypes during fluctuating light will be necessary for developing strategies to improve  $C_4$  crop performance. Additionally, low-growth-light intensity increases steady-state  $\phi$  of shaded field-grown *M. × giganteus* leaves, assuming the  $C_i$  in the bundle sheath is much higher than  $C_i$  in the  $\phi$  estimation (Kromdijk *et al.*, 2008). Although the underlying basis of the increased  $\phi$  in shade-adapted leaves may be different from the increased  $\phi$  in fluctuating light, these leakages could be additive, which would further handicap the efficiency of leaves within  $C_4$  canopies. We demonstrated a new experimental design with the TDL to estimate  $\phi$  at high resolution and under transient conditions. This technique provides opportunities to investigate further the underlying causes of increased  $\phi$ , as well as facilitating strategies to improve  $C_4$  plant performance in fluctuating light.

#### A new experimental design for the TDL with a gas-exchange system

The coupling of a TDL with a gas-exchange system has been used to measure leakiness in  $C_4$  plants under photosynthetic steady-state conditions (Pengelly *et al.*, 2010; Ubierna *et al.*, 2011, 2013). Recent work has coupled gas-exchange systems to a TDL to measure mesophyll conductance during induction curves (Sakoda *et al.*, 2021; Liu *et al.*, 2022); however, these studies were only able to estimate mesophyll conductance every 120 s over the activation curve. Our method, allowing the TDL to remain on the leaf chamber for 600 s, enabled us to have a nearly continuous high-resolution (10 s) dataset over a 30 min high-light induction. This allowed the measurement of  $\phi$  under nonsteady-state conditions. The stability and precision of the instrument are critical to the accuracy of the estimation of  $\phi$  (Fig. N1 in Notes S1). The error of our laser could be controlled within a limited range during the experiment, and the averaging time of 10 s significantly reduced the system noise and improved the prediction accuracy, with sufficient time resolution for the purposes of the questions asked in this study (Notes S1, laser performance). In the first *c.* 100 s of the induction, the error associated with  $\Delta^{13}C_{\text{obs}}$  estimation was > 50%, which indicated that our measurements were masked by instrument error. Thus, we minimized our interpretation of the leakiness values in this time frame. The error associated with photosynthetic discrimination ( $\Delta^{13}C_{\text{obs}}$ ) was < 30% after 200 and 130 s for sorghum and maize, respectively, indicating that the error associated with the TDL was acceptable for the remainder of the induction. The error associated with the laser can change through time, environment and with retuning of the laser. These

characters were verified for each laser and tested before each application. As  $CO_2$  concentration around Rubisco ( $C_{bs}$ ) should not be much higher than  $CO_2$  in mesophyll ( $C_m$ ) at the beginning of the induction, the complete calculation of leakiness (Eqn 12) was used instead of the simplified model that assumes the  $C_{bs}$  is much higher than  $C_m$  (Fig. S7). Additionally, we developed a program to calculate the leakiness automatically from raw carbon isotope and gas-exchange data, which improved throughput of data analysis.

The accuracy of the measured gas-exchange values was significantly improved by correcting for the time delay of the system (Figs S8, S9). The measuring noise of carbon isotope mole fractions was also constrained by averaging signals within every 10 s (Fig. N1 in Notes S1), and thus the noise in leakiness estimation was also reduced (Fig. S2), although the accuracy of the measurement was still limited by the precision of the gas-exchange system and the TDL in the first *c.* 100 s after the illumination. We expect that our measurement experience and data-processing program will help researchers to save time and develop new applications for this system.

#### Acknowledgements

The sorghum work was supported by the DOE Center for Advanced Bioenergy and Bioproducts Innovation (US Department of Energy, Office of Science, Office of Biological and Environmental Research under award no. DE-SC0018420) and the maize work by the project Realizing Increased Photosynthetic Efficiency (RIPE), which is funded by the Bill & Melinda Gates Foundation, Foundation for Food and Agriculture Research (FFAR) and the UK Foreign, Commonwealth and Development Office, under grant no. OPP1172157. We thank Amanda P. de Souza, Jeff Hansen, Wei Wei, Elena Pelech, Elsa De Becker, Cindy Kher Xing Chan, Yi Xiao and Benjamin Haas for their comments and advice on earlier versions of this manuscript. We also thank Dr Nerea Ubierna for helpful comments on previous drafts.

#### Author contributions

The project was conceived by YW, SSS and SPL. YW and SSS performed the experiments. YW developed the data-processing tool and analyzed the data. SSS developed the method for continual monitoring of leakage through induction. CJB and SSS set up the TDL. YW, SSS and SPL wrote the manuscript with insights from DRO, RAB and CJB. YW and SSS contributed equally to this work.

#### ORCID

Carl J. Bernacchi  <https://orcid.org/0000-0002-2397-425X>  
 Ryan A. Boyd  <https://orcid.org/0000-0003-4009-7700>  
 Stephen P. Long  <https://orcid.org/0000-0002-8501-7164>  
 Donald R. Ort  <https://orcid.org/0000-0002-5435-4387>  
 Samantha S. Stutz  <https://orcid.org/0000-0002-3999-9726>  
 Yu Wang  <https://orcid.org/0000-0002-6951-2835>

## Data availability

The data and code that support the findings of this study are available at doi: [10.13012/B2IDB-1181155\\_V1](https://doi.org/10.13012/B2IDB-1181155_V1).

## References

- Acevedo-Siaca LG, Coe R, Wang Y, Kromdijk J, Quick WP, Long SP. 2020. Variation in photosynthetic induction between rice accessions and its potential for improving productivity. *New Phytologist* 227: 1097–1108.
- Acevedo-Siaca LG, Dionora J, Laza R, Paul Quick W, Long SP. 2021. Dynamics of photosynthetic induction and relaxation within the canopy of rice and two wild relatives. *Food and Energy Security* 10: e286.
- Ashton A, Burnell J, Hatch M. 1984. Regulation of C<sub>4</sub> photosynthesis: inactivation of pyruvate, Pi dikinase by ADP-dependent phosphorylation and activation by phosphorolysis. *Archives of Biochemistry and Biophysics* 230: 492–503.
- Barbour MM, McDowell NG, Tcherkez G, Bickford CP, Hanson DT. 2007. A new measurement technique reveals rapid post-illumination changes in the carbon isotope composition of leaf-respired CO<sub>2</sub>. *Plant, Cell & Environment* 30: 469–482.
- Bellasio C, Griffiths H. 2014. Acclimation to low light by C<sub>4</sub> maize: implications for bundle sheath leakiness. *Plant, Cell & Environment* 37: 1046–1058.
- Bellasio C, Quirk J, Buckley TN, Beerling DJ. 2017. A dynamic hydro-mechanical and biochemical model of stomatal conductance for C<sub>4</sub> photosynthesis. *Plant Physiology* 175: 104–119.
- Bowling DR, Sargent SD, Tanner BD, Ehleringer JR. 2003. Tunable diode laser absorption spectroscopy for stable isotope studies of ecosystem–atmosphere CO<sub>2</sub> exchange. *Agricultural and Forest Meteorology* 118: 1–19.
- Brown RH, Byrd GT. 1993. Estimation of bundle sheath cell conductance in C<sub>4</sub> species and O<sub>2</sub> insensitivity of photosynthesis. *Plant Physiology* 103: 1183–1188.
- Burnell JN, Chastain CJ. 2006. Cloning and expression of maize-leaf pyruvate, Pi dikinase regulatory protein gene. *Biochemical and Biophysical Research Communications* 345: 675–680.
- von Caemmerer S. 2000. *Biochemical models of leaf photosynthesis*. Collingwood, Australia: CSIRO Publishing.
- von Caemmerer S, Evans JR, Hudson GS, Andrews TJ. 1994. The kinetics of ribulose-1, 5-bisphosphate carboxylase/oxygenase *in vivo* inferred from measurements of photosynthesis in leaves of transgenic tobacco. *Planta* 195: 88–97.
- von Caemmerer S, Farquhar GD. 1981. Some relationships between the biochemistry of photosynthesis and the gas exchange of leaves. *Planta* 153: 376–387.
- von Caemmerer S, Furbank RT. 2016. Strategies for improving C<sub>4</sub> photosynthesis. *Current Opinion in Plant Biology* 31: 125–134.
- von Caemmerer S, Ghannoum O, Pengelly JJ, Cousins AB. 2014. Carbon isotope discrimination as a tool to explore C<sub>4</sub> photosynthesis. *Journal of Experimental Botany* 65: 3459–3470.
- Carmo-Silva AE, Salvucci ME. 2013. The regulatory properties of Rubisco activase differ among species and affect photosynthetic induction during light transitions. *Plant Physiology* 161: 1645–1655.
- Crafts-Brandner SJ, Salvucci ME. 2000. Rubisco activase constrains the photosynthetic potential of leaves at high temperature and CO<sub>2</sub>. *Proceedings of the National Academy of Sciences, USA* 97: 13430–13435.
- Craig H. 1953. The geochemistry of the stable carbon isotopes. *Geochimica et Cosmochimica Acta* 3: 53–92.
- De Souza AP, Wang Y, Orr DJ, Carmo-Silva E, Long SP. 2020. Photosynthesis across African cassava germplasm is limited by Rubisco and mesophyll conductance at steady state, but by stomatal conductance in fluctuating light. *New Phytologist* 225: 2498–2512.
- De Wet J. 1978. Special paper: systematics and evolution of Sorghum sect. Sorghum (Gramineae). *American Journal of Botany* 65: 477–484.
- Deans RM, Farquhar GD, Busch FA. 2019. Estimating stomatal and biochemical limitations during photosynthetic induction. *Plant, Cell & Environment* 42: 3227–3240.
- Degen GE, Orr DJ, Carmo-Silva E. 2021. Heat-induced changes in the abundance of wheat Rubisco activase isoforms. *New Phytologist* 229: 1298–1311.
- Dohleman FG, Long SP. 2009. More productive than maize in the Midwest: how does *Miscanthus* do it? *Plant Physiology* 150: 2104–2115.
- Edwards G, Walker D. 1983. *C<sub>3</sub>, C<sub>4</sub>: mechanisms, cellular and environmental regulation of photosynthesis*. Oxford, UK: Blackwell Scientific.
- Evans JR, von Caemmerer S. 2013. Temperature response of carbon isotope discrimination and mesophyll conductance in tobacco. *Plant, Cell & Environment* 36: 745–756.
- FAO, IFAD, UNICEF, WFP, WHO. 2020. *The state of food security and nutrition in the World 2020. Transforming food systems for affordable healthy diets*. Rome, Italy: FAO.
- Farquhar GD. 1983. On the nature of carbon isotope discrimination in C<sub>4</sub> species. *Functional Plant Biology* 10: 205–226.
- Farquhar GD, Cernusak LA. 2012. Ternary effects on the gas exchange of isotopologues of carbon dioxide. *Plant, Cell & Environment* 35: 1221–1231.
- Hatch MD. 1978. Regulation of enzymes in C<sub>4</sub> photosynthesis. *Current Topics in Cellular Regulation* 14: 1–27.
- Hatch MD. 1987. C<sub>4</sub> photosynthesis: a unique blend of modified biochemistry, anatomy and ultrastructure. *Biochimica et Biophysica Acta (BBA) – Reviews on Bioenergetics* 895: 81–106.
- Henderson SA, Caemmerer S, Farquhar GD. 1992. Short-term measurements of carbon isotope discrimination in several C<sub>4</sub> species. *Functional Plant Biology* 19: 263–285.
- Hubbart S, Ajigboye OO, Horton P, Murchie EH. 2012. The photoprotective protein PsbS exerts control over CO<sub>2</sub> assimilation rate in fluctuating light in rice. *The Plant Journal* 71: 402–412.
- Jaikumar NS, Stutz SS, Fernandes SB, Leakey AD, Bernacchi CJ, Brown PJ, Long SP. 2021. Can improved canopy light transmission ameliorate loss of photosynthetic efficiency in the shade? An investigation of natural variation in *Sorghum bicolor*. *Journal of Experimental Botany* 72: 4965–4980.
- Kaiser E, Morales A, Harbinson J, Heuvelink E, Prinzenberg AE, Marcelis LF. 2016. Metabolic and diffusional limitations of photosynthesis in fluctuating irradiance in *Arabidopsis thaliana*. *Scientific Reports* 6: 1–13.
- Keeley JE, Rundel PW. 2003. Evolution of CAM and C<sub>4</sub> carbon-concentrating mechanisms. *International Journal of Plant Sciences* 164(S3): S55–S77.
- Kim SY, Slattery RA, Ort DR. 2021. A role for differential Rubisco activase isoform expression in C<sub>4</sub> bioenergy grasses at high temperature. *GCB Bioenergy* 13: 211–223.
- Kromdijk J, Schepers HE, Albanito F, Fitton N, Carroll F, Jones MB, Finnan J, Lanigan GJ, Griffiths H. 2008. Bundle sheath leakiness and light limitation during C<sub>4</sub> leaf and canopy CO<sub>2</sub> uptake. *Plant Physiology* 148: 2144–2155.
- Kromdijk J, Ubierna N, Cousins AB, Griffiths H. 2014. Bundle-sheath leakiness in C<sub>4</sub> photosynthesis: a careful balancing act between CO<sub>2</sub> concentration and assimilation. *Journal of Experimental Botany* 65: 3443–3457.
- Kubásek J, Urban O, Šantrůček J. 2013. C<sub>4</sub> plants use fluctuating light less efficiently than do C<sub>3</sub> plants: a study of growth, photosynthesis and carbon isotope discrimination. *Physiologia Plantarum* 149: 528–539.
- Lanigan GJ, Betson N, Griffiths H, Seibt U. 2008. Carbon isotope fractionation during photorespiration and carboxylation in *Senecio*. *Plant Physiology* 148: 2013–2020.
- Lee MS, Boyd RA, Ort DR. 2022. The photosynthetic response of C<sub>3</sub> and C<sub>4</sub> bioenergy grass species to fluctuating light. *GCB Bioenergy* 14: 37–53.
- Liu T, Barbour MM, Yu D, Rao S, Song X. 2022. Mesophyll conductance exerts a significant limitation on photosynthesis during light induction. *New Phytologist* 233: 360–372.
- Long SP, Marshall-Colon A, Zhu X-G. 2015. Meeting the global food demand of the future by engineering crop photosynthesis and yield potential. *Cell* 161: 56–66.
- Long SP, Spence AK. 2013. Toward cool C<sub>4</sub> crops. *Annual Review of Plant Biology* 64: 701–722.
- Long SP, Taylor SH, Burgess SJ, Carmo-Silva E, Lawson T, DeSouza A, Leonelli L, Wang Y. 2022. Into the shadows and back into sunlight: photosynthesis in fluctuating light. *Annual Reviews of Plant Biology* 73: 617–648.

- McAusland L, Murchie EH. 2020. Start me up; harnessing natural variation in photosynthetic induction to improve crop yields. *New Phytologist* 227: 989–991.
- McAusland L, Violet-Chabrand S, Davey P, Baker NR, Brendel O, Lawson T. 2016. Effects of kinetics of light-induced stomatal responses on photosynthesis and water-use efficiency. *New Phytologist* 211: 1209–1220.
- Mook W, Bommerson J, Staverman W. 1974. Carbon isotope fractionation between dissolved bicarbonate and gaseous carbon dioxide. *Earth and Planetary Science Letters* 22: 169–176.
- Mott KA, Woodrow IE. 2000. Modelling the role of Rubisco activase in limiting non-steady-state photosynthesis. *Journal of Experimental Botany* 51(Suppl 1): 399–406.
- Murchie EH, Ruban AV. 2020. Dynamic non-photochemical quenching in plants: from molecular mechanism to productivity. *The Plant Journal* 101: 885–896.
- Ohkubo S, Tanaka Y, Yamori W, Adachi S. 2020. Rice cultivar Takanari has higher photosynthetic performance under fluctuating light than Koshihikari, especially under limited nitrogen supply and elevated CO<sub>2</sub>. *Frontiers in Plant Science* 11: 1308.
- Ozeki K, Miyazawa Y, Sugiura D. 2022. Rapid stomatal closure contributes to higher water use efficiency in major C<sub>4</sub> compared to C<sub>3</sub> Poaceae crops. *Plant Physiology* 189: 188–203.
- Pearcy RW. 1990. Sunflecks and photosynthesis in plant canopies. *Annual Review of Plant Biology* 41: 421–453.
- Pearcy RW. 1994. Photosynthetic utilization of sunflecks: a temporally patchy resource on a time scale of seconds to minutes. In: Caldwell MM, Pearcy RW, eds. *Exploitation of environmental heterogeneity by plants*. San Diego, CA, USA: Academic Press, 175–208.
- Pengelly JJ, Sirault XR, Tazoe Y, Evans JR, Furbank RT, von Caemmerer S. 2010. Growth of the C<sub>4</sub> dicot *Flaveria bidentis*: photosynthetic acclimation to low light through shifts in leaf anatomy and biochemistry. *Journal of Experimental Botany* 61: 4109–4122.
- Qiao M-Y, Zhang Y-J, Liu L-A, Shi L, Ma Q-H, Chow WS, Jiang C-D. 2021. Do rapid photosynthetic responses protect maize leaves against photoinhibition under fluctuating light? *Photosynthesis Research* 149: 57–68.
- Sage RF. 2004. The evolution of C<sub>4</sub> photosynthesis. *New Phytologist* 161: 341–370.
- Sage RF, Sage TL, Kocacinar F. 2012. Photorespiration and the evolution of C<sub>4</sub> photosynthesis. *Annual Review of Plant Biology* 63: 19–47.
- Sakoda K, Yamori W, Groszmann M, Evans JR. 2021. Stomatal, mesophyll conductance, and biochemical limitations to photosynthesis during induction. *Plant Physiology* 185: 146–160.
- Sakoda K, Yamori W, Shimada T, Sugano SS, Hara-Nishimura I, Tanaka Y. 2020. Higher stomatal density improves photosynthetic induction and biomass production in Arabidopsis under fluctuating light. *Frontiers in Plant Science* 11: 1609.
- Slattery RA, Walker BJ, Weber AP, Ort DR. 2018. The impacts of fluctuating light on crop performance. *Plant Physiology* 176: 990–1003.
- Taylor SH, Gonzalez-Escobar E, Page R, Parry MA, Long SP, Carmo-Silva E. 2022. Faster than expected Rubisco deactivation in shade reduces cowpea photosynthetic potential in variable light conditions. *Nature Plants* 8: 118–124.
- Taylor SH, Long SP. 2017. Slow induction of photosynthesis on shade to sun transitions in wheat may cost at least 21% of productivity. *Philosophical Transactions of the Royal Society of London. Series B: Biological Sciences* 372: 20160543.
- Tazoe Y, Von Caemmerer S, Estavillo GM, Evans JR. 2011. Using tunable diode laser spectroscopy to measure carbon isotope discrimination and mesophyll conductance to CO<sub>2</sub> diffusion dynamically at different CO<sub>2</sub> concentrations. *Plant, Cell & Environment* 34: 580–591.
- Ubierna N, Holloway-Phillips M-M, Farquhar GD. 2018. Using stable carbon isotopes to study C<sub>3</sub> and C<sub>4</sub> photosynthesis: models and calculations. In: Covshoff S, ed. *Photosynthesis: methods in molecular biology*. New York, NY, USA: Humana Press, 155–196.
- Ubierna N, Sun W, Cousins AB. 2011. The efficiency of C<sub>4</sub> photosynthesis under low light conditions: assumptions and calculations with CO<sub>2</sub> isotope discrimination. *Journal of Experimental Botany* 62: 3119–3134.
- Ubierna N, Sun W, Kramer DM, Cousins AB. 2013. The efficiency of C<sub>4</sub> photosynthesis under low light conditions in *Zea mays*, *Miscanthus x giganteus* and *Flaveria bidentis*. *Plant, Cell & Environment* 36: 365–381.
- Wang Y, Burgess SJ, de Becker EM, Long SP. 2020. Photosynthesis in the fleeting shadows: an overlooked opportunity for increasing crop productivity? *The Plant Journal* 101: 874–884.
- Wang Y, Chan KX, Long SP. 2021. Toward a dynamic photosynthesis model to guide yield improvement in C<sub>4</sub> crops. *The Plant Journal* 107: 343–359.
- Wingate L, Seibt U, Moncrieff JB, Jarvis PG, Lloyd J. 2007. Variations in <sup>13</sup>C discrimination during CO<sub>2</sub> exchange by *Picea sitchensis* branches in the field. *Plant, Cell & Environment* 10: 600–616.
- Woodrow IE, Mott KA. 1993. Modeling C<sub>3</sub> photosynthesis – a sensitivity analysis of the photosynthetic carbon reduction cycle. *Planta* 191: 421–432.
- Yang CJ, Samayoa LF, Bradbury PJ, Olukolu BA, Xue W, York AM, Tuholski MR, Wang W, Daskalska LL, Neumeyer MA. 2019. The genetic architecture of teosinte catalyzed and constrained maize domestication. *Proceedings of the National Academy of Sciences, USA* 116: 5643–5652.
- Zhu X-G, Long SP, Ort DR. 2008. What is the maximum efficiency with which photosynthesis can convert solar energy into biomass? *Current Opinion in Biotechnology* 19: 153–159.
- Zhu X-G, Long SP, Ort DR. 2010. Improving photosynthetic efficiency for greater yield. *Annual Review of Plant Biology* 61: 235–261.
- Zhu XG, Ort DR, Whitmarsh J, Long SP. 2004. The slow reversibility of photosystem II thermal energy dissipation on transfer from high to low light may cause large losses in carbon gain by crop canopies: a theoretical analysis. *Journal of Experimental Botany* 55: 1167–1175.

## Supporting Information

Additional Supporting Information may be found online in the Supporting Information section at the end of the article.

**Fig. S1** Pictures of the setup for the two gas-exchange systems used for the measurements.

**Fig. S2** Increasing the time averaged for each data point from 1 to 10 s significantly limited the estimation noise of the leakiness.

**Fig. S3** The [CO<sub>2</sub>] of Li-Cor 6400 opaque conifer chamber and Li-Cor 6800 large leaf chamber (CO<sub>2</sub>S) changes with the decrease of influx [CO<sub>2</sub>] (CO<sub>2</sub>R) from 800 to 400 μmol mol<sup>-1</sup>.

**Fig. S4** A semilogarithmic plot of the difference between the net CO<sub>2</sub> assimilation (*A*) and steady-state net CO<sub>2</sub> assimilation at 1800 μmol m<sup>-2</sup> s<sup>-1</sup> (*A<sub>f</sub>*) as a function of time.

**Fig. S5** Estimated bundle-sheath leakiness, Δ<sup>13</sup>C<sub>obs</sub> and ξ during photosynthetic induction of maize B73 calculated from tunable diode laser absorption spectroscopy coupled to a gas-exchange system (LI-6800).

**Fig. S6** Bundle-sheath leakiness during photosynthetic induction of maize B73 and sorghum Tx430.

**Fig. S7** Estimated φ<sub>is</sub> is and φ<sub>i</sub> during photosynthetic induction of sorghum and maize.

**Fig. S8** Time correction of CO<sub>2</sub> assimilation and bundle-sheath leakiness during photosynthetic induction of sorghum.

**Fig. S9** Time correction of CO<sub>2</sub> assimilation and bundle-sheath leakiness during photosynthetic induction of maize.

**Methods S1** Correction of the system delay.

**Notes S1** Performance of tunable diode laser absorption spectroscopy.

**Table S1** Estimated values of leakiness and CO<sub>2</sub> assimilation rate (*A*) of each individual sorghum plant.

**Table S2** Estimated values of leakiness and CO<sub>2</sub> assimilation rate (*A*) of each individual maize plant.

Please note: Wiley Blackwell are not responsible for the content or functionality of any Supporting Information supplied by the authors. Any queries (other than missing material) should be directed to the *New Phytologist* Central Office.